Journal of. Modern Trends in Physics Research
Online ISSN 2636-4220
DOI: 10.19138/mtpr/(14)73-80
Accepted: 2014-12-19

Growth of layered wedge-shaped islands of Pb on the vicinal Si: new mechanism of twin boundary formation

S. I. Bozhko[1], A. S. Ksyonz[1,3], A. M. Ionov[1], D. A. Fokin[1,2], V. Dubost[2], F. Debontridder[2], T. Cren[2] and D. Roditchev[2]

[1] *Institute of Solid States Physics, RAS, Chernogolovka, Moscow district, 142432, Russia.*
[2] *Institute des Nanosciences de Paris, UMR 75 88 au C.N.R.S., University Paris 6 UPMC, Paris, France.*
[3] *Lomonosov Moscow State University, Faculty of Fundamental Physical and Chemical Engineering, 119991, Moscow, Russia.*

Abstract- The growth of Pb on a clean vicinal Si(557) surface at room temperature was studied using the Scanning Tunneling Microscopy. We observed anisotropic tilted wedge-shaped Pb-islands to grow following the Stransky-Krastanov scenario. The elongation of the islands along the step edges of Si is associated with the anisotropic potential of the vicinal template. The observed peculiar slab-like stacking morphology of the formed wedge-shaped islands is discussed considering the substrate-induced strain, twin formation and the energy of the electron gas confined inside the islands.

1. INTRODUCTION

Nanometer scale Pb-islands stir up a current burst of studies of both quantum electronic effects and strongly confined superconductivity [1]. In those studies the Si(111)-(7x7) reconstructed surface is often used as a substrate for the Pb growth, allowing the control of the size and shape of the Pb-nano-islands but also, of their thickness due to the electronic growth (EG) regime. The EG model based on quantum size effect (QSE) [2, 3] was proposed to explain the nature of metallic film growth on different substrates [4]; Pb on Si(111) is one of the systems where the QSE is revealed. Indeed, the layer-by-layer mode (Frank-van der Merve) realized there at low temperatures (< 95K) [5] is replaced at higher temperatures by a layer-plus-island mode (Stranski-Krastanov) [6] where QSE is displayed [4, 7-19].

Pb film growth on Si(111) starts from a wetting layer formation. Its thickness was reported to be 3 mono-layers (ML) [13], 2ML [8] or 1ML [14]. For thicknesses exceeding 1.22ML the wetting layer is highly disordered [20, 21]. Separate bulk Pb islands start to grow on the wetting layer in a very specific way: The island height increases by "steps" of 2ML following so-called bi-layer growth [12-15]. Statistically, the islands with odd number of MLs are predominant. Moreover, it was shown that the islands of 7Ml thickness are markedly privileged [7-11, 16-19].

The formation of the islands with flat tops and steep edges along with their peculiar height distribution cannot be easily explained in terms of classical growth. The EG explains such a growth mode [4, 7, 16-17] considering the electron gas confined in a two-dimensional quantum well (QW) of the width defined by the Pb island thickness. The confinement results in oscillations of the electron energy as a function of island thickness. For thicknesses from 4 to 10ML, the electron gas energy displays an absolute minimum for 7ML Pb islands [17]. With further increasing the thickness, the odd-thickness energy gain decreases and vanishes at a "magic" thickness corresponding to 10ML; above 10ML the even ML numbers become preferable [14, 17-19]. The dependence of energy oscillations on the QW width can be influenced by the boundary conditions [17]. The island height distribution can also be influenced by the substrate surface structure [22-24].

The multilayer films grown on vicinal Si surfaces have not yet been thoroughly studied. The Si(557) surface is well known to be an atomically ordered step array. The surface was widely investigated in a large variety of experiments [25-32]. It was shown that the clean Si(557) surface forms a regular triple step staircase with a period of 5.73 nm which can potentially be used as an atomically accurate length standard [27, 31] or a diffraction lattice for soft X-rays. When grown on such a surface the Pb films should reveal some additional aspects of the island growth, due to the symmetry of vicinal surfaces, different from Si(111) (7x7). The Pb growth on such surfaces was previously studied in [33-36], but no information about islands structure in the real space was reported.

Journal of. Modern Trends in Physics Research
Online ISSN 2636-4220
DOI: 10.19138/mtpr/(14)73-80
Accepted: 2014-12-19

Here we report on Scanning Tunneling Microscopy (STM) studies of the growth of Pb on Si(557) surface. Tilted wedge-shaped Pb islands are observed elongated along the step edges of the vicinal Si. The experimental data and specifically, the slab-like island stacking are analyzed and discussed considering the substrate-induced strain, possible twin formation and the energy of the electron gas confined in the islands.

2. EXPERIMENT

The experiment was carried in our home made UHV system ($P<10^{-10}$ Torr) at INSP combining in-situ sample preparation facility, LEED, Auger Spectroscopy and STM [37]. Precise calibration of the STM was done at room temperature using constant current mode imaging of large (50-300nm) single atomic step terraces of Si(111)-(7x7); the calibration was verified on atomic steps present in thick Pb-islands grown on Si(111). Tungsten STM tips were prepared by electrochemical etching in 2M NaOH followed by ultrasonic bath treatment in distilled water and pure ethanol. The tips were degassed in UHV by heating up to 600˚C for several hours. They were then heated by direct current up to 1000-1200°C prior using them in STM experiment.

The surface of Si(557) samples was prepared as following [25, 26]. First both, the sample and sample holder were degassed at 600ºC until the residual gas pressure in the chamber went down to~3×10^{-10} Torr. Then the sample was cooled down to room temperature in 2-3 hours. Then, the sample was flashed to 1200ºC for 60s by direct current flowed perpendicularly to the step edges, cooled down to 900ºC in 30 s where it was maintained for 60 s. Finally, the sample was slowly cooled down to room temperature. The resulting sample surface showed no contamination when analyzed by Auger Electron Spectroscopy, while LEED revealed the characteristic diffraction pattern of vicinal Si [26]. The STM measurements have demonstrated that the surface was regular and didn't contain any bunch structures other than triple steps, in agreement with [25]. After the clean Si surface was prepared, Pb was deposited using an e-beam evaporator. During the Pb deposition the temperature of the substrate was kept at 300K, the pressure was in the range of 2×10^{-10} Torr. The nominal amount of Pb deposited on the surface was about 16ML.

3. RESULTS AND DISCUSSIONS

3.1. *Structure of Si(557) substrate.*

The atomic structure of the Si(557) surface has been reported in numerous publications and was demonstrated to be very sensitive to the surface preparation procedure [25]. Moreover, our STM experiments revealed that different macroscopic regions of the same nominally Si(557) oriented samples could reveal the (557), (7 7 10) or (223) periodic staircase structures altered by (111)-(7x7) regions [25, 26, 29]. Importantly, (557), (7 7 10) and (223) consist of a regular array of triple steps and Si(111)-(7x7) terraces with the periodicity of 5.73nm, 5.39nm and 4.74nm, respectively [25, 29, 30, 31]. The surface energy of those vicinal surfaces are close, hence, the realization of a particular structure can be caused by the presence of a small amount of defects at the surface [25]. In all cases, the terrace planes coincide with Si(111), and the step height corresponds well to the triple interplanar atomic spacing in the [111] direction of the Si. The Si(111)-(7x7) structure was routinely resolved on (111) facets of (557), (7 7 10) and (223) regions. As an example, Fig.1. presents STM images of a nominally Si(557) oriented sample showing large areas covered by (7 7 10) triple step structure in (a) and Si(111)-(7x7) reconstruction resolved on Si(111) terraces in (b) [30].

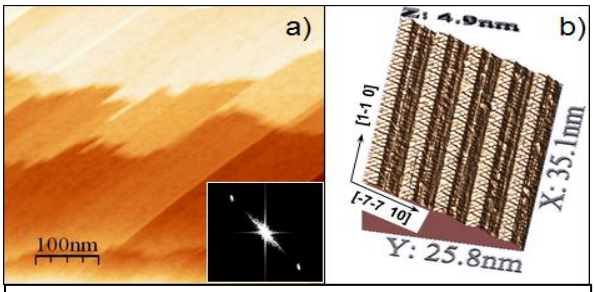

Fig.1. STM images of the clean Si(557) surface showing in (a): large areas covered with Si(7 7 10) stepped structure; in (b): 3D-plot of the triple step structure with (7x7)-reconstruction on Si(111) terraces. Inset : Fast Fourier Transformation of (a) reveals two characteristic peaks at the frequency corresponding to the (7 7 10) stepped structure.

Nominal Si(557) surfaces were also investigated by LEED [26]. The kinematical approximation analysis demonstrates that diffraction pattern contains three modulations caused by the periodicity of a regular step staircase, the presence of triple step structure and Si(111)-(7x7) surface reconstruction.

Journal of. Modern Trends in Physics Research
Online ISSN 2636-4220
DOI: 10.19138/mtpr/(14)73-80
Accepted: 2014-12-19

3.2. *Growth of Pb on Si(7 7 10) stepped surface*

The first stage of Pb growth both on the Si(111)-(7x7) [14, 15, 17, 20, 38] and on vicinal planes close to Si(111) [35, 36] consists in the formation of a smooth Pb wetting layer. At the second stage, three-dimensional Pb-islands are formed, in agreement with the Stransky-Krastanov scenario [6]: Their small inclination of about 1° with respect to the Si(111) has already been determined by LEED [36], but the morphology and structure was not reported so far. A typical STM image acquired just after Pb deposition is shown in Fig.2a. The surface consists of a number of islands elongated in the direction parallel to the step edges. Between the islands a stepped structure is observed (Figs.2a,c,d); its periodicity is exactly the one of the Si(7 7 10) surface (Fig.2c) [39].

A zoom on an island-free area (Fig.2b) allows one to analyze the structure of the wetting layer which appears anisotropic and consists of stripes along the [-110] direction. The corrugation in the direction [-5-5 7] normal to the step edges is periodic with a typical period of about 5.3nm (Fig.2c, top curve), thus coinciding with the periodicity of the triple stepped structure observed on clean Si(7 7 10) [25, 26] (Fig.2c, bottom curve). The corrugation in this direction was found to be about 0.15nm. The image cross-section taken along the step edge direction [-110] (Fig.3e) reveals a weak modulation of 0.05nm in height with a period of about 5.6nm, close to the double of the (7×7) unit cell (the latter being observed on the terraces, Fig. 1). As a result, the apparent roughness of the Pb-wetting layer is about 0.04nm RMS, whereas it is of about 0.15nm for the clean Si(7 7 10) stepped surface. This means that the wetting layer somehow smoothes the surface as compared to the clean Si(7 7 10). The effect is clearly seen in Fig.2c. The detailed analysis shows that Pb atoms preferentially fill the bottom of the triple steps of Si(7 7 10) surface (individual decorating Pb atoms are resolved there, Fig.2b), just few atoms cover the (7x7) terraces. This effect is clearly related to the anisotropic potential of the stepped surface on which highly mobile Pb adatoms move. To identify the exact Pb atom positions, further low temperature STM experiments are necessary. In any case, the mechanism of the wetting layer formation on the Si(557), (7 7 10) or (223) surface clearly differs from the case of Si(111) where a continuous amorphous 1-3ML thick wetting layer is formed [36].

The presence of steps induces the anisotropic diffusion of Pb-atoms on Si(557) and influences the wetting layer formation but also, puts serious constraints on the island growth. In particular, the presence of steps is responsible of their peculiar elongated shape in the [-110] direction (Fig.2b,f). Moreover, the cross section **d** taken in [-5-5 7] direction, Fig.2d, shows that the island top layers are not parallel to the substrate plane Si(7 7 10). Owing to the careful calibration of our STM we were able to measure quite precisely the angles that the top layer of individual islands forms with respect to the nominal crystallographic plane (7 7 10) of the substrate. We found in all cases a tilt of 9.1°±0.4° (the accuracy being limited by the creep of the piezo-tube of our STM). At the same time, the angle between crystallographic planes (7 7 10) and (111) is 10.02°. This means that the flat top of the islands is tilted by about 1° with respect to the Si(111) plane. Note, that the same misorientation value was observed in LEED study of Pb grown on Si(557) staircase [36].

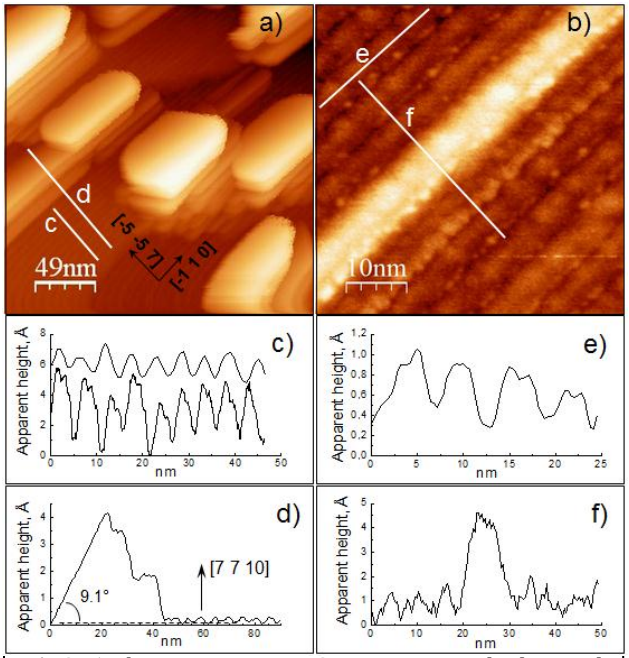

Fig.2. a) The constant current STM image reveals elongated wedge-shaped layered Pb islands grown on vicinal Si; b) STM image of the wetting layer obtained on an island-free area; c) The height modulation of the clean vicinal Si(7 7 10) triple step structure (bottom curve) compared to that of the wetting layer covered surface (top curve - section **c** in a)); d) The flat top of Pb-islands is tilted by 9.1°±0.4° with respect to the substrate (7 7 10) plane - section **d** in a); e) The periodicity of the wetting layer at Si(111) terraces matches the size of the (7x7) unit cell - section **e** in b); f) At first stages, wire-like Pb-islands grow separately on Si(111) terraces - section **f** in b).

To clarify the island morphology we represent in Fig.3a the same image as in Fig.2a but after the subtraction of a tilted plane allowing the flat tops of the Pb islands to appear parallel to the image plane. Despite the inevitable tip convolution effects, one clearly sees that the island flat tops are truncated triangles, allowing one to determine their precise crystallographic orientation. Importantly, two kinds of islands were observed depending on their flat top orientations: the ones with their [-110] parallel to the [-110] direction of

Journal of. Modern Trends in Physics Research
Online ISSN 2636-4220
DOI: 10.19138/mtpr/(14)73-80
Accepted: 2014-12-19

the substrate and the others, anti-parallel oriented. The islands of the second kind are turned by 180° around Pb[111] axis with respect to those of the first kind.

The cross-section **b** presented in Fig.3b clearly demonstrates the overall triangular section of Pb islands. The sides of the triangle are: the base Si(7 7 10), flat top Pb(111) plane tilted by about 9° from the (7 7 10) substrate (red dashed line) as discussed above, and the third, rough side with the average direction close to Pb[113], as the arrow in Fig.3b indicates. This rough side consists of a series of nanometer scale steps (Fig.3b).

The statistical analysis of the rough sides of different islands evidenced the existence of preferable step heights of about 2nm (7 Pb MLs). Indeed, Fig.3d presents the height distribution histograms of two selected areas, marked 1 and 2 in Fig.3a, each belonging to the rough side of a single Pb island. The top plane of the lower terrace of each island was taken as the baseplate. From the position of the peaks on the histograms it becomes clear that the most of terraces seen in the areas 1 and 2 are separated in height by about 2nm. The histograms also reveal the presence of layers with other thicknesses (marked with arrows) but they are statistically rare. A larger statistics is given in the histogram (Fig.4f) of the step height distribution in the rough side regions of 12 different Pb islands, taken from several STM images. A clear maximum at 2nm indicates that the rough side regions have Pb(111) terraces with the preferential step height coinciding with the most stable 7ML thick Pb island structure observed on Si(111) and explained by EG model as discussed in introduction. Note that the 2nm thick terraces extend continuously to other neighboring sides of the islands, where they finally reach the substrate. These terraces make one think about possible 2nm-thick slab structure of Pb islands (quite evident in the Pb(111)-projected images, Figs.3a and 4a).

Let us analyze now the way the Pb(111) flat top plane is connected to the vicinal substrate on a thin side of Pb islands. The cross-sections by a (1-10) plane (Figs.3c, 4b-e) display three different encountered situations. In Fig.4d the flat island top is directly attached to the stepped substrate. In Figs. 3c, 4c the top slab of about 2nm is disconnected, while the underlying slab is connected. Third, for some islands a thicker layer is completely disconnected from the stepped surface (Figs.4b,e). This thicker layer corresponds in fact to a 2nm thick top slab sitting on a partially connected block. It means that, similarly to the thick side, the thin side island "connection" to the substrate is also quantized in units of 2nm-thick slabs.

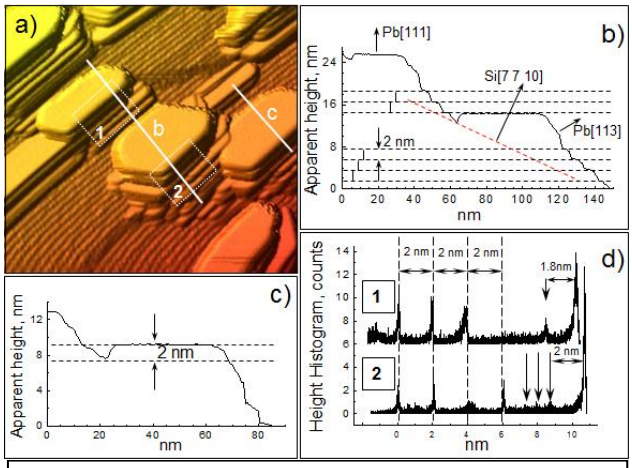

Fig.3. a) STM image of the Pb film with the drawing plane coinciding with the Pb(111) island top surface; b) Plot of the cross section **b** in a). The red dashed line corresponds to the (7 7 10) substrate. c) Cross-section **c** of a) reveals the layered structure of the island; d) Histograms of the heights in the areas 1 and 2 in a) reveal the existence of characteristic step heights of 2nm.

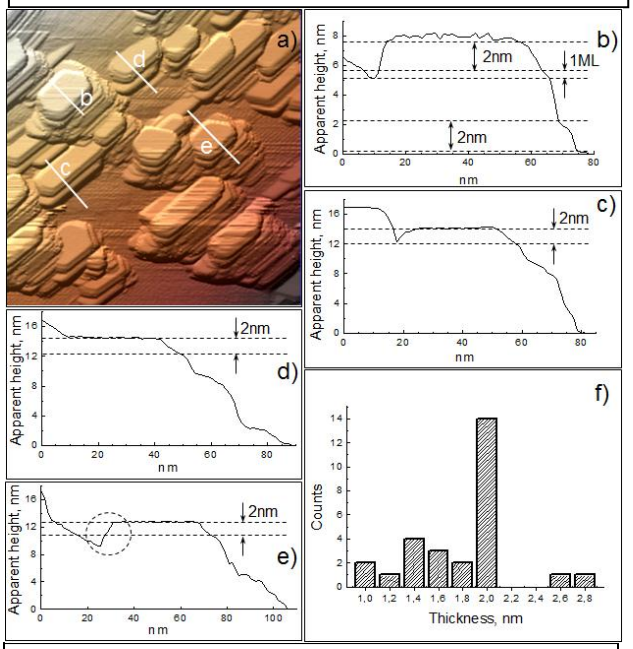

Fig.4. a) A 500nm x 500nm STM image of Pb film on Si(7 7 10) surface (tilted as in Fig.3a); b)-e): Cross sections **b-e** of different Pb-islands in a); f) The layer thickness statistics obtained from 12 different Pb-islands.

4. DISCUSSION

Let us discuss few possible mechanisms that may explain such specific Pb island morphology observed on (7 7 10) triple stepped vicinal surface. At the beginning, small Pb wire-like islands are formed independently on different Si(111) terraces, with the triple step as the nucleation zone (Fig.2b,f). With increasing the amount of Pb atoms, these

Journal of. Modern Trends in Physics Research
Online ISSN 2636-4220
DOI: 10.19138/mtpr/(14)73-80
Accepted: 2014-12-19

islands reach 3ML thickness. The islands occupying neighboring Si(111) terraces start to overlap, and the incommensurability between the Si(7 7 10) substrate structure and bulk Pb becomes essential. First of all, the thickness of the Pb(111) 3ML, 3x0.286nm=0.858nm, is lower than the Si(111) triple step, 3x0.313nm=0.939nm. Second, the atomic structures of Pb islands growing on neighboring Si(111) terraces are initially not in phase because the 5.39nm period of the Si(7 7 10) structure is not commensurate with Pb(111) parameters. These heights and phase mismatches cause the strain accumulation at the Pb/Si interface and result in a strained growth of Pb islands. This interfacial strain is only partially relaxed by tilting the Pb(111) with respect to Si(111) by about 1°, as indeed observed by LEED [36] and confirmed by our STM data. This tilt corresponds to the adjustment of the height difference of 0.081nm, accumulated over the 5.39nm period of the Si(7 7 10) stepped structure. In thin islands the initial strain is not relaxed, and the strain energy is simply proportional to the island volume. The stratification of the islands in slabs would be an additional way to release the strain and relax the lattice of the growing Pb crystal. However, this energy gain is imbalanced by a supplementary energy contribution proportional to the total surface of inter-layer boundaries created in the island.

In order to evaluate the total energy balance one also has to take into account the energy of the electron gas confined in a thin island. In the usual EG model the electron gas is considered as confined in a two-dimensional quantum well. As discussed in the introduction, in the case of Pb on Si(111) the well width corresponds to the thickness of a flat Pb island. According to [17], the energy for such a gas is:

$$E_s = A(N)\sin\left(2k_F^{bulk}Nt + \varphi\right) + B \;;$$

where ***A*** is the amplitude parameter, ϕ is the phase shift factor, k_F^{bulk} is the Fermi wave vector for bulk Pb, ***N×t*** is the quantum well width, ***N*** being the number of interlayers spacings ***t***=2.86Å and ***B*** is an offset constant.

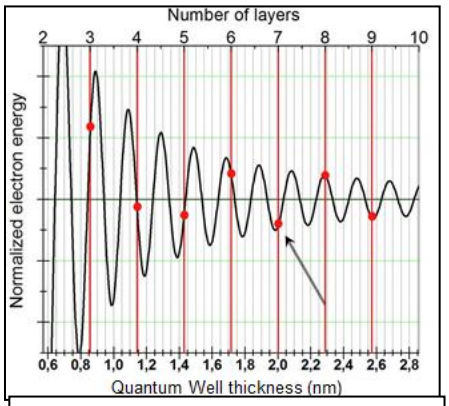

Fig.5. The energy of the electron gas confined in the infinite quantum well calculated as a function of the well thickness (curve). The energy is plotted with respect to the electron gas energy in the bulk (taken as origin). Vertical red lines note the situation corresponding to integer number of monolayers of Pb. Red dots: corresponding electron gas energy.

Fig.5 shows the dependence of the electron gas energy on the width of an infinite barrier quantum well. The energy oscillates as a function of the well thickness and, in the thick limit, it coincides with Fermi energy for a bulk Pb crystal (***Ef***). The thickness of real Pb islands is discrete: it is equal to ***N×t***. Corresponding ***N+1*** values are shown as vertical red lines in Fig.5; the realistic situations (integer number of MLs) are represented by red dots. Fig.5 shows that if the quantum well is 7 ML wide, the two-dimensional electron gas energy value indeed exhibits a local minimum: Among the red dots in Fig.5 the one corresponding to 7ML (marked by arrow) has the lowest energy position. We note that the thicknesses of 3ML, 6ML and 8ML are not favorable from the point of view of electron energy. Remarkably, the thickness of 7 ML is the most energetically favorable one, even with respect to the bulk material. Thus, the electron energy of a Pb island divided in slabs of 7ML is lower than the electron energy of a bulk single crystal of the same size and shape. Such stratification, however, has an important energy cost since the boundaries should be created inside Pb islands. A twin boundary seems to be one of the most favorable candidates for Pb islands [40].

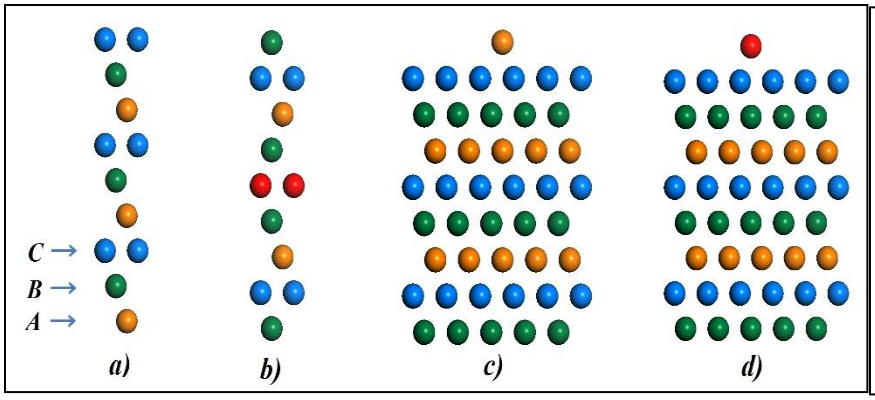

Fig.6. Side view of model structures of Pb nanoislands used in DFT simulations. a) model of perfect structure 8 ML in thick; b) model of nanoisland which contains twin boundary at the middle (marked in red); c) model of individual atom deposited onto Pb nanoisland surface in ***fcc*** position; d) model of individual atom deposited onto Pb nanoisland surface in ***hcp*** position.

Journal of. Modern Trends in Physics Research
Online ISSN 2636-4220
DOI: 10.19138/mtpr/(14)73-80
Accepted: 2014-12-19

To make the stratification possible, the gains in the electron energy ΔE_e realized upon division should exceed the total energy of the created twin boundaries ΔE_{TB}. In order to evaluate the energy, gain due to stratification of the nanoislands we performed the model calculations of a total energy of Pb structures in a frame of DFT approximation. The slabs of model structures were separated by a vacuum gap of >20A° in the z direction, sampled by a 8×8×1 mesh in k space. The calculations were carried out using plane-wave DFT with the PBEsol density functional (Materials Studio, Castep Accelrys). Fig.6a demonstrates model structure of perfect Pb slab (referred as "perfect structure"). Positions of Pb atoms in the slab are the same as in a bulk of Pb crystal with the lattice constant of 5.04 A. FCC crystal structure of Pb can be described in terms of a sequence of 3 types of hexagonal close packed monolayers A, B, C marked in yellow, green and blue respectively. Except of position in z direction A, B, C monolayers are shifted one from other in x-y plain. Another slab (Fig. 6b) contains twin boundary at the middle (referred as "TB structure"). Fig. 7a represents dependence of energy of perfect structure E_S as a function of a slab thickness. The oscillations observed at small thickness are due to QSE in a good agreement with Fig.5 and [17, 46]. Quantum confinement effect ceases if the slab thickness exceeds 20ML. To separate the contribution of creation of twin boundaries ΔE_{TB} the calculations were performed using slabs thick enough to avoid effect of quantum confinement. ΔE_{TB} was determined as a difference in total energies of TB structure and perfect structure. Using the slab 41nm in thick as a model structure ΔE_{TB} was found to be of 14meV/atom. Concerning ΔE_{TB}, previous studies performed on small nanoparticles revealed a structure which is characterized by multiple twinned domains in many ***fcc*** metals [41-43] and especially in Pb [39]. Most of the studied particle configurations (>90%) are characterized by the existence of twins. Twin structures are mainly single and multiple twins - up to 5 twins. At room temperature a twin structure of particles is not stable for particle sizes of <10nm, twin structure fluctuates in time [40]. However, the lifetime of the configuration increases with the particle size, from about 0.04 sec for 4 nm particles, up to long term stability for particles with a diameter larger than 10 nm. Energy of stacking fault was estimated to be of 26meV.

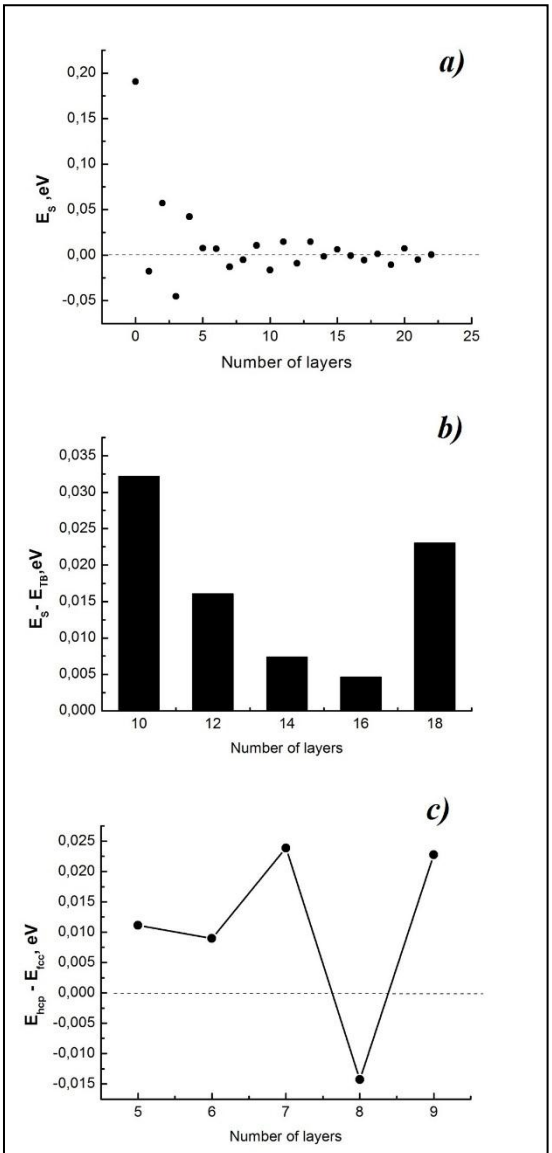

Fig.7. a) dependence of energy of perfect structure E_S as a function of a slab thickness; b) dependence of difference in total energies of TB structure E_{TB} and perfect structure E_S on a slab thickness; c) difference in total energies of ***hcp*** and ***fcc*** structures E_{hcp}-E_{fcc} is plotted as a function of a slab thickness.

QSE in TB structure were studied at d<20ML. Fig.7b demonstrates dependence of difference in total energies of TB structure E_{TB} and perfect structure E_S on a slab thickness. The dependence reveals minimum of 4meV/atom at 14-16ML i.e. 4nm in thick. The tb structure 4nm in thick consists of two slabs 7ML in thick each separated by twin boundary. Energy gain due to quantum confinement can be estimated as E_{TB}-E_S-ΔE_{TB}=10meV. However, the energy gain of the electron system per surface atom for individual nanoisland 7 ML in thick was measured to be ~-30 meV [17]. One could simplistically expect the energy gain enlarged roughly by a factor of two compared to that of the individual nanoisland 7 ML in thick, if the twin boundary is considered as nontransperent. Of course, the twin boundary does not reflect the conduction electrons very efficiently [44, 45], and ΔE_e has to be reduced by the transparency constant.

Nevertheless, even being positive in the minimum of total energy balance, the ΔE_e term is small in comparison with kT. Therefore both TB structure and perfect structure are almost equivalent in energy. In order to simulate formation of twin boundary, model structures presented in Fig. 6c, d were used. The ***fcc*** structure (Fig.6c) corresponds to position of extra atom on the surface when perfect ***fcc*** crystal structure is growing up. Growth via ***hcp*** structure (Fig.6d) resulted

Journal of. Modern Trends in Physics Research
Online ISSN 2636-4220
DOI: 10.19138/mtpr/(14)73-80
Accepted: 2014-12-19

in a formation of twin boundary. In Fig 7c difference in total energies of ***hcp*** and ***fcc*** structures E_{hcp}-E_{fcc} is plotted as a function of a slab thickness. Formation of a twin boundary is favorable in energy only for a slab 7 ML in thick. This fact could satisfactory explains the observed formation of the 7ML thick pancake-like structures. Besides, the experimental observation of differently oriented flat tops of Pb islands in our study is consistent with the appearance of twins for which the orientation of successive slabs should alternate.

5. SUMMARY

In this paper we have studied the growth of Pb-islands on the vicinal Si(7 7 10) surface. We have found that the growth of Pb on this periodic structure, consisting of (7x7)-reconstructed Si(111) terraces and triple Si-steps, follows in general the Stransky-Krastanov scenario. First, an ultra-thin wetting layer covers the substrate and makes the morphology of the vicinal stepped structure smoother. After that, separate wedge-shaped Pb islands are formed, elongated in the [-110] direction. The Pb(111)-oriented islands are found tilted with respect to Si(111) by approximately 1°, due to the Pb/Si lattice mismatch. The interfacial strain is suggested to partially relax owing the generation of twin boundaries separating the islands into two-dimensional slabs appearing in the STM images. The statistical analysis evidenced the existence of the characteristic thickness (2nm) of those slabs, corresponding exactly to 7 Pb monolayers. We argue that such growth mode is realized due to the minimization of the electron energy owing to the quantum confinement inside the created quantum wells. Thus, the growth mechanism can be explained in the framework of the EG model including the interfacial strain and twin boundary formation.

ACKNOWLEDGEMENTS

The work was partially supported by Russian Academy of Sciences ("New materials and Structures", Program №24 "Basic technologies of Nanostructures and Nanomaterials"), and the Ministry of Education and Science of the Russian Federation. STM images were processed and presented using WSXM software [47].

REFERENCES

1. T. Nishio, T. An, A. Nomura, K. Miyachi, T. Eguchi, H. Sakata, S. Lin, N. Hayashi, N. Nakai, M. Machida, Y.Hasegawa, Phys. Rev. Lett. **101,** 167001 (2008), C.Brun, I-P. Hong, F. Patthey, I.Yu. Sklyadneva, R. Heid, P. M. Echenique, K. P. Bohnen, E.V. Chulkov, W.-D. Schneider Phys. Rev. Lett. **102**, 207002 (2009), W. H. Choi, H. Koh, E. Rotenberg, H. W. Yeom, Phys. Rev. B **75**, 075329 (2007), J. H. Dil, T. U. Kampen, B. Hülsen, T. Seyller, K. Horn, Phys. Rev. B **75**, 161401(R) (2007), D. Eom, S. Qin, M.-Y. Chou, C. K. Shih, Phys. Rev. Lett. **96**, 027005 (2006), S. Qin, J. Kim, Q. Niu, C.-K. Shih, Science, **324**, 1314 (2009)
2. Peter J.Feibelman, D.R.Hamann, Phys. Rev. B, **29**, 12, (1984)
3. Jian Wang, Xu-Cun Ma, Yun Qi, Ying-Shuang Fu, Shuai-Hua Ji, Li Lu, Jin-Feng Jia, Qi-Kun Xue, Appl. Phys. Lett., **90**, 113109 (2007)
4. Zhenyu Zhang, Qian Niu, and Chih-Kang Shih, Phys. Rev. Lett. **80**, 5381 (1998)
5. M. Jalochowski, M.Hoffman and E. Bauer, Phys. Rev. B, **51**, 7231 (1995)
6. Ivan N. Stranski and L. Von Krastanow, Abhandlungen der Mathematisch-Naturwissenschaftlichen Klasse. Akademie der Wissenschaften und der Literatur in Mainz, **146**, 797, (1939)
7. L. L. Wang, X. C. Ma, P. Jiang, Y. S. Fu, S. H. Ji, J. F. Jia, and Q. K. Xue, Phys. Rev. B, **74,** 073404 (2006)
8. K. Budde, E. Abram, V. Yeh, and M. C. Tringides, Phys. Rev. B, **61**, R10602 (2000)
9. S. H. Chang, W. B. Su, W. B. Jian, C. S. Chang, L. J. Chen, and Tien T. Tsong, Phys. Rev. B, **65**, 245401 (2002)
10. V. Yeh, L. Berbil-Bautista, C. Z. Wang, K. M. Ho, and M. C. Tringides Phys. Rev. Lett., **85**, 5158 (2000)
11. J. H. Dil, T. U. Kampen, B. Hülsen, T. Seyller, and K. Horn, Phys. Rev. B **75**, 161401R (2007)
12. Shao-Chun Li, Xucun Ma, Jin-Feng Jia, Yan-Feng Zhang, Dongmin Chen, Qian Niu, Feng Liu, Paul S. Weiss and Qi-Kun Xue, Phys. Rev. B **74**, 075410 (2006)
13. I. B. Altfeder, K. A. Matveev and D. M. Chen, Phys. Rev. Lett. **78**, 2815 (1997)
14. Hawoong Hong, C.-M.Wei, M.Y. Chou, Z.Wu, L. Basile, H. Chen, M. Holt, and T.-C. Chiang, Phys. Rev. Lett. **90**, 076104 (2003)
15. Z. Kuntova, M. Hupalo, Z. Chvoj, M.C. Tringides, Surf. Sci. **600**, 4765–4770 (2006)
16. W. B. Su, S. H. Chang, W. B. Jian, C. S. Chang, L. J. Chen, and Tien T. Tsong, Phys. Rev. Lett. **86**, 5116 (2001)

17. P. Czoschke, Hawoong Hong, L. Basile, and T.-C. Chiang, Phys. Rev. B **72**, 075402 (2005)
18. Yan-Feng Zhang, Jin-Feng Jia, Zhe Tang, Tie-Zhu Han, Xu-Cun Ma, Qi-Kun Xue, Surf. Sci. **596**, L331-L338 (2005)
19. Yan-Feng Zhang, Jin-Feng Jia, Tie-Zhu Han, Zhe Tang, Quan-Tong Shen, Yang Guo, Z. Q. Qiu, and Qi-Kun Xue1, Phys. Rev. Lett. **95**, 096802 (2005)
20. M. Jalochowski and E. Bauer, J. Appl. Phys. **63**, 4501(1988)
21. H.H.Weitering, D.R.Heslinga, T.Himba, Phys. Rev. B, **45** 5991 (1992)
22. R. Zdyb, Appl. Surf. Sci., **254** 4408–4413 (2008)
23. M.Hupalo, S.Kremmer, V.Yeh, L.Berbil-Bautista, E.Abram, M.C.Tringides, Surf. Sci., **493,** 526 (2001) and references there in
24. R. Feng, E.H. Conrad, M.C. Tringides, C. Kim and P.F. Miceli Appl. Phys. Lett., **85**, 3866 (2004)
25. A.N. Chaika, D.A. Fokin, S.I. Bozhko, A.M. Ionov, F.Debontridder, V.Dubost, T.Cren and D. Roditchev, J. Appl. Phys, **105**, 034304 (2009),
26. A.N. Chaika, D.A. Fokin, S.I. Bozhko, A.M. Ionov, F.Debontridder, T.Cren and D. Roditchev, Surf. Sci., **603**, 752 (2009)
27. J. Viernow, J.-L. Lin, D. Y. Petrovykh, F. M. Leibsle, F. K. Men and F. J. Himpsel Appl. Phys. Lett., **72**, 948 (1998)
28. J.-L. Lin, D. Y. Petrovykh, J. Viernow, F. K. Men, D. J. Seo and F. J. Himpsel, Appl. Phys. Lett., **84**, 255 (1998)
29. S.A. Teys, K.N. Romanyuk, R.A. Zhachuk, B.Z. Olshanetsky, Surf. Sci. **600**, 4878-4882 (2006)
30. Jian Wei, X.-S. Wang, J. L. Golberg, N. C. Bartelt, and Ellen D.Williams, Phys. Rev. Lett. **68**, 3885 (1992)
31. A. Kirakosian, R. Bennewitz, J. N. Crain, Th.Fauster, J.-L. Lin, D. Y. Petrovykh, and F. J. Himpsel, Appl. Phys. Lett. **79**, 1608 (2001)
32. M. Henzler, R. Zhachuk, Thin Solid Films **428**, 129–132 (2003)
33. C. Tegenkamp, J. Phys.: Condens. Matter 21, 013002 (2009)
35. M Czubanowski, A Schuster, S Akbari, H Pfnür and C Tegenkamp, New Journal of Physics, **9**, 338 (2007)
36. C. Tegenkamp, H. Pfnür, Surf. Sci. **601**, 2641–2646 (2007)
37. E. Hoque, A. Petkova, M. Henzler Surf. Sci. **515**, 312–322 (2002)
38. T. Cren, F. Debontridder, D. Fokin, V. Dubost and D. Roditchev. «New STM Facility in Paris :Ultra-low Temperature, High Magnetic Fields, Ultra-high Vacuum STM/STS with in-situ Growth and Surface Characterization». Cryoconference 2008, 8-13 september 2008, Miraflores de la Sierra (Madrid), Spain.
39. H. H. Weitering, D. R. Heslinga, and T. Hibma, Phys. Rev B **45**, 5991 (1992). In the manuscript we present the growth on Si(7 7 10) staircase substrate, but the same growth scenario should hold for other triple stepped structures such as Si(557) and Si(223).
40. T. Ben-David, Y. Lereah, G. Deutscher, J. M. Penisson, A. Bourret R. Kofman, P. Cheyssac, Phys.Rev.Lett. **78**, 2585 (1997)
41. S. Ino, J. Phys. Soc. Jpn. **21**, 346(1966)
42. J. G. Allpress and J. V. Sanders, Surf. Sci. **7**, 1 (1967).
43. K. Kimoto and I. Nishida, J. Phys. Soc. Jpn. **22**, 940 (1967).
44. Yu.V. Sharvin and D. Yu. Sharvin Sov. Phys. JETP **50**, 1033 (1979)
45. Tsoi M.V., Böhm A., Primke M., Tsoi V.S., and Wyder P. Phys. Rev.B **56**, R15581 (1997)
46. Miao Liu, Yong Han, Lin Tang, Jin-Feng Jia, Qi-Kun Xue, and Feng Liu, Phis Rev B **86**, 125427 (2012)
47. I. Horcas, R. Fernandez, J.M. Gomez-Rodriguez, J. Colchero, J. Gomez-Herrero, and A.M. Baro, Rev. Sci. Instrum. 78, 013705 (2007).